Measuring large numerical apertures by imaging the angular distribution of radiation of fluorescing molecules

Luru Dai,[1,2] Ingo Gregor,[1] Iris von der Hocht,[1] Thomas Ruckstuhl,[3] Jörg Enderlein[1]

[1]*Institute for Biological Information Processing 1 Forschungszentrum Jülich 52425 Jülich, Germany*
j.enderlein@fz-juelich.de

[2]*Interdisciplinary Center of Theoretical Studies The Institute of Theoretical Physics, Chinese Academy of Sciences, Beijing 100080 P. R. China*
dailuru@itp.ac.cn

[3]*National Centre for Sensor Research, Dublin City University, Dublin 9, Ireland*
thomas.ruckstuhl@dcu.ie

Abstract: Exact knowledge of the numerical aperture is crucial in many applications using high-aperture objectives such as confocal microscopy, optical trapping, or advanced sub-wavelength imaging methods. We propose and apply a precise and straightforward method for measuring this fundamental parameter of microscope objectives with numerical apertures above unity. Our method exploits the peculiarities of the fluorescence emission of molecules at a glass/air interface.

OCIS codes: (110.1220) Apertures; (110.0180) Microscopy; (170.1790) Confocal microscopy.

References

1. P.M. Goodwin, W.P. Ambrose, R.A. Keller "Single-molecule detection in liquids by laser-induced fluorescence," Acc. Chem. Res. **29**, 607-613 (1996).
2. J. Enderlein, M. Böhmer "Fluorescence spectroscopy of single molecules under ambient conditions: Methodology and technology," Chem. Phys. Chem. **4**, 792-808 (2003).
3. R. Rigler, J. Widengren "Ultrasensitive Detection of single molecules by fluorescence correlation spectroscopy," Bioscience **3**, 180-183 (1990).
4. P. Schwille "Fluorescene correlation spectroscopy and its potential for intracellular applications," Cell Biochem. Biophys. **34**, 383-408 (2001).
5. A. Ashkin "Optical Trapping And Manipulation Of Neutral Particles Using Lasers," Proc. Nat. Acad. Sci. **94**, 4853-4860 (1997).
6. K.C. Neuman, S.M. Block "Optical Trapping," Rev. Sci. Instrum. **75**, 2787-809 (2004).
7. D.R. Sandison, D.W. Piston, R.M. Williams, W.W. Webb "Quantitative comparison of background rejection, signal-to-noise ratio, and resolution in confocal and full-field laser scanning microscopes," Appl. Opt. **34**, 3576-3588 (1995).
8. D.W. Piston "Choosing objective lenses; The importance of numerical aperture and magnification," Biol. Bull. **195**, 1-4 (1998).
9. S.W. Hell, H.K. Stelzer "Properties of a 4Pi confocal fluorescence microscope," J. Opt. Soc. Am. A **9**, 2159-2166 (1992).
10. T.A. Klar, S.W. Hell "Subdiffraction resolution in far-field fluorescence microscopy," Opt. Lett. **24**, 954-956 (1999).
11. A. Schönle, S.W. Hell "Calculation of vectorial three-dimensional transfer functions in large-angle focusing systems," J. Opt. Soc. Am. A **19**, 2121-2126 (2002).
12. Neto P.A. Maia, H.M. Nussenzveig "Theory of optical tweezers" Europhys. Lett. **50**, 702-708 (2000).
13. C.J.R. Sheppard, M., Kawata Y. Gu, S. Kawata "Three-dimensional transfer functions for high-aperture systems," J. Opt. Soc. Am. A **11**, 593-598 (1994).

#8730 - $15.00 USD Received 7 September 2005; revised 31 October 2005; accepted 3 November 2005

14. M. Böhmer, J. Enderlein "Orientation imaging of single molecules by wide-field epi-fluorescence microscopy," J. Opt. Soc. Am. B **20,** 554-559 (2003).
15. J. Enderlein, I. Gregor, D. Patra, T. Dertinger, B. Kaupp "Performance of fluorescence correlation spectroscopy for measuring diffusion and concentration," Chem. Phys. Chem. (2005) in press.
16. M. Müller, G.J. Brakenhoff "Characterization of high-numerical-aperture lenses by spatial autocorrelation of the focal field," Opt. Lett. **20**, 2159-2162 (1995).
17. R. Juškaitis "Characterizing High Numerical Aperture Microscope Objective Lenses" in: *Optical Imaging and Microscopy*, Eds.: P. Török ad F.-J. Kao (Springer, 2003) pp. 21-43.
18. W. Lehmann, A. Wachtel "Numerical apertures of light microscope objectives," J. Microsc. **169**, 89-90 (1993).
19. W. Lukosz "Light emission by multipole sources in thin layers. I. Radiation patterns of electric and magnetic dipoles," J. Opt. Soc. Am. **71**, 744-754 (1981).
20. J. Enderlein, T. Ruckstuhl, S. Seeger "Highly Efficient Optical Detection of Surface-Generated Fluorescence," Appl. Opt. **38**, 724-732 (1999).
21. W. Schroeyers, R. Vallee, D. Patra, J. Hofkens, S. Habuchi, T. Vosch, M. Cotlet, K. Müllen, J. Enderlein, F.C. De Schryver "Fluorescence Lifetimes and Emission Patterns Probe the 3D Orientation of the Emitting Chromophore in a Multichromophoric System," J. Am. Chem. Soc. **126**, 14310-14311 (2004).
22. D. Patra, I. Gregor, J. Enderlein "Image Analysis of Defocused Single-Molecule Images for Three-Dimensional Molecule Orientation Studies," J. Phys. Chem. A **108,** 6836-6841 (2004).

1. Introduction

The numerical aperture (NA) of a microscope objective is one of its most crucial characteristics. It defines the maximum angle of incidence when focusing light, and the maximum angle of light collection when detecting light or imaging. Objectives with high numerical aperture play a central role in applications where focusing of light to a minimum possible spot and maximum light collection efficiency are desired. Applications include single-molecule fluorescence spectroscopy [1,2], fluorescence correlation spectroscopy [3,4], optical trapping [5,6], multiphoton excitation and ultra high resolution microscopy [7,8]. Another important application is epi-fluorescence total-internal reflection microscopy (objective-type TIRFM), which uses a high-NA objective, not only for light detection but also for TIRF excitation by sending a laser beam into the objective above the critical angle of total internal reflection between glass and the sample solution (usually water). Advanced optical imaging methods, such as 4Pi microscopy [9] or stimulated emission depletion (STED) microscopy [10], also need objectives with as large a numerical aperture as possible for achieving highest imaging resolution. In all of these applications, precise knowledge of the numerical aperture is highly desirable for correctly modelling the experimental set-ups and their performance [11-13] or for correctly evaluating measurement results [14,15].

There are several methods for measuring the numerical aperture of objectives. The most advanced and technically complex methods are based on interference measurements [16,17], yielding not only information about the NA but also on image quality and potential aberrations. The necessary technology for performing such measurements is not widely distributed and is restricted to optical industry institutions or research facilities that specialise in pure and applied optics. A much simpler method for NA measurements was described by Lehmann and Wachtel [18] and is based on measuring divergence angles of light rays in the conjugate space of an objective. Although the method is simple, its precision relies on the accuracy with which light-ray angles can be measured. Here, we propose a straightforward and easy-to-implement method that uses the intrinsic physics of the emission of fluorescing molecules at a glass/air interface. The method is robust, self-referencing and does not need any further knowledge of the optical properties of the measured objective (such as magnification). It works for any aplanatic objective (i.e. one that obeys Abbe's sine condition) and for all NA values larger than one. It is thus perfectly suited for characterizing high-NA objectives. The method is accurate to 10^{-2} in NA-value.

#8730 - $15.00 USD Received 7 September 2005; revised 31 October 2005; accepted 3 November 2005

2. Theoretical background

From an electrodynamic point of view, most fluorescing molecules behave as perfect electric dipole emitters. Thus, when embedded within a dielectrically homogenous environment, the angular distribution of their emission follows the classical $\sin^2\theta$-law of a Hertz dipole emitter, where θ is the angle between the dipole's axis and the chosen direction of emission. This behavior alters dramatically when a molecule is placed close to an interface between two media with different dielectric properties, e.g. a glass/air interface. Due to the self-interaction of the dipole with its own emission that is back-reflected from the interface, its angular distribution of emission is significantly modified. A detailed theoretical treatment of these modifications can be found in refs.[19,20]. In the present context, the most important point is that the emission into the optically denser medium shows a prominent discontinuity at the angle of total internal reflection between the two media,

$$\theta_{TIR} = \mathrm{asin}(n_0/n), \tag{1}$$

where n and n_0 are the refractive indices of the two media ($n_0 < n$). This is visualized in Fig. 1(a), where the angular distribution of emission is shown for a large number of randomly oriented molecules in glass at a glass/air interface. This corresponds to molecules immobilized in a thin polymer layer with a refractive index of glass, deposited onto glass in air. When imaging this emission with an aplanatic, infinity-corrected objective, this angular distribution of emission is converted into a circular intensity distribution in the back-focal plane of the objective.

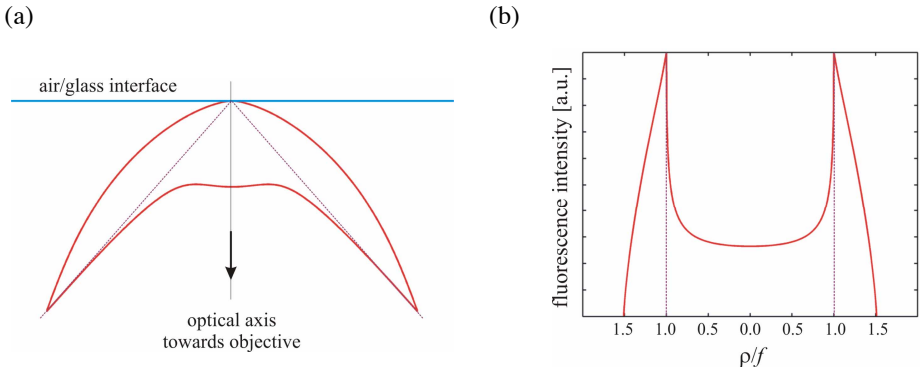

Fig. 1. (a) Angular distribution of emission into glass for isotropically oriented molecules in glass at an air/glass interface when excited by light circularly polarized within the plane of the interface. Emission maximum occurs at the angle of total internal reflection (TIR), indicated by light-red lines. (b) Intensity distribution of fluorescence within the back focal plane of an objective as a function of the distance ρ from the optical axis divided by the focal distance f of the objective. The vertical light-red lines show the position of TIR.

For an aplanatic objective, there exists a linear relationship between the sine of the angle of emission emanating from the objective's focus θ and the radius ρ in the back focal plane of the objective, given by

$$\rho = f\, n \sin\theta \tag{2}$$

where f is the focal length of the objective, and n is the refractive index of the immersion medium. Thus, if the objective were to collect light over the complete solid angle of the glass half space, the angular distribution of emission would be converted into an intensity distribu-

#8730 - $15.00 USD Received 7 September 2005; revised 31 October 2005; accepted 3 November 2005

tion over the back-focal plane as shown in Fig. 1(b). However, the NA of the objective sets an upper limit to the collection angle, which leads to an abrupt cut-off of the observed intensity distribution in the back-focal plane at some maximum radius, ρ_{max}. The important point is that the discontinuity in the angular distribution of light occurs always at the angle of total internal reflection between air and glass and thus corresponds to a numerical aperture of ~ 1.00 (refractive index of air). If we denote the radius where this discontinuity is observed in the back focal plane by ρ_{TIR}, one directly finds that the numerical aperture of an objective is given by

$$NA = \rho_{max} / \rho_{TIR} \tag{3}$$

There are several remarkable points that make this method of determining a NA so attractive. First, in an experiment, the fluorescent molecules are usually not situated only within an infinitely thin layer directly at the interface, but embedded within a polymer layer of finite thickness. However, even for a distribution of molecules within a layer of sub-wavelength but finite thickness, the sharp discontinuity in fluorescence emission at the TIR angle will still be there. Second, if the molecules are not isotropically oriented within the layer, it will change the shape of the curves in Fig. 1, but the discontinuity will still remain at the TIR angle. Third, the exact value of the refractive index of the glass is also of no importance, because the position of the emission discontinuity always corresponds to a numerical aperture equal to the refractive index of air. Thus, the proposed method is self-referencing and robust. The method is also applicable to non-infinity corrected objectives, as long as the objective obeys Abbe's sine condition so that there is a linear relationship between radial position of light rays at the back exit pupil of the objective and their incidence angle in front of the objective, θ.

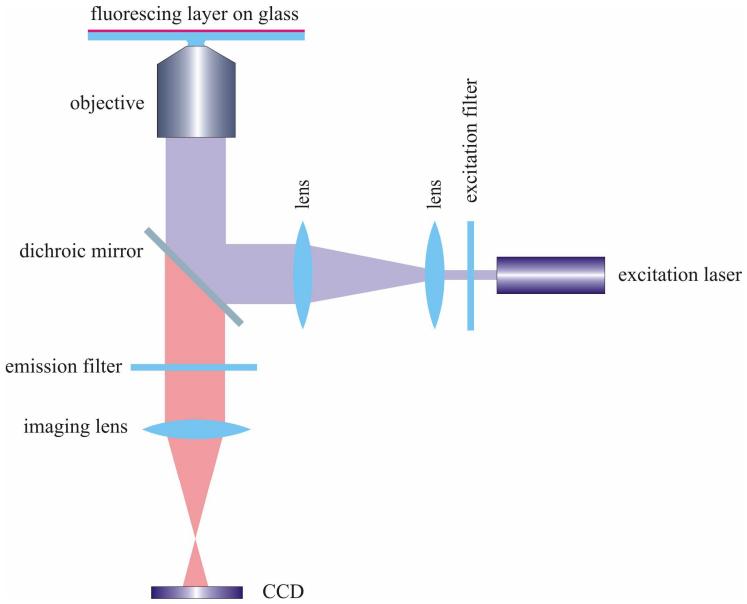

Fig. 2. Principal scheme of the experimental set-up used for imaging the intensity distribution of fluorescence in the back focal plane of the objective. The imaging lens images the back focal plane of the objective onto the CCD camera. In the realized experimental set-up, this imaging was achieved by using the microscope's tube lens (not shown) plus and additional lens.

#8730 - $15.00 USD Received 7 September 2005; revised 31 October 2005; accepted 3 November 2005

3. Experiment

The measurement set-up is shown in Fig. 2. The light of an Ar^+-ion laser of 514.5 nm wavelength is collimated and tightly focused through the studied objective and matching immersion medium onto a glass slide covered with a thin layer of polymer (polymethylmetacrylate, PMMA) containing a high concentration of the fluorescing dye tetramethylrhodamine (TMR). This layer was generated by spin-coating a solution of the dye-doped polymer in methanol onto the cover-slide, generating a polymer layer thickness below 100 nm. The fluorescence collected by the objective results in an intensity distribution in its back focal plane, which is imaged by two lenses (tube lens, IX 71 by Olympus, 180 mm focal length, and an achromat with a 100 mm focal length, Linos) onto a sensitive CCD camera (iXon DV885, Andor). Exposure time per image was on the order of 5 s and the overall excitation intensity was set to 100 µW. The focus diameter on the sample surface was estimated to be below 5 µm.

4. Results and discussion

We measured five different oil immersion and water immersion objectives from Olympus. For each objective, the measurement was repeated 10 times. Two typical images of the intensity distributions within the back focal plane are shown in Fig. 3.

(a) (b)

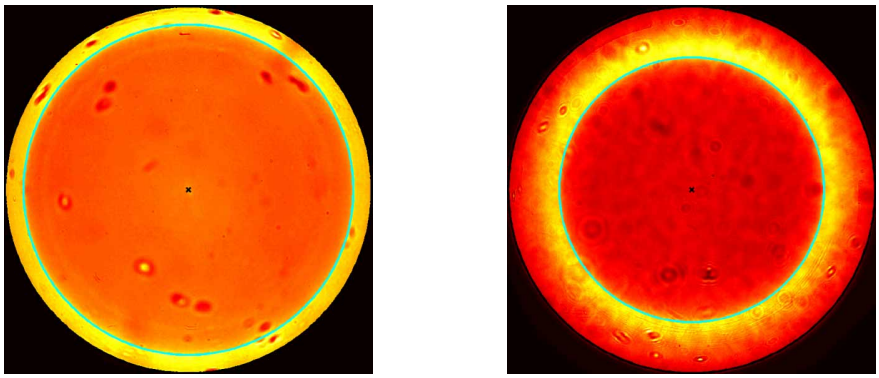

Fig. 3. (a) Measured intensity distribution in the back focal plane for the Olympus UApo/340 40× objective with nominal NA of 1.15. The barely visible black circle at the edge of the illuminated area is the determined out NA-determined cut-off of fluorescence collection, the cyan circle marks the position of the fluorescence discontinuity at the TIR-angle. (b) Same as Fig. 3(a), but for the Olympus PlanApo 60× objective with nominal NA of 1.4.

The cut-off of fluorescence collection was determined as the position of steepest decline of fluorescence intensity at the edge of the illuminated area. The position of the intensity-distribution discontinuity (cyan circles) was determined by fitting a calculated intensity distribution to that area taking into account a finite thickness of the fluorescent polymer layer with unknown dye distribution and orientation. The determined values of the NA are listed in Table 1 together with the objectives' names and nominal NA values. The standard deviation of the measured NA was determined on the basis of ten measurements. As can be seen, the objectives with large NA nearly perfectly meet the design specifications. The largest deviations between nominal and measured NA occur for the 1.2 and 1.3 NA objectives. This is in agreement with previous experiments where these objectives were used for defocused imaging and the best correspondence between measured and calculated defocused single

#8730 - $15.00 USD Received 7 September 2005; revised 31 October 2005; accepted 3 November 2005

ing and the best correspondence between measured and calculated defocused single molecules images were obtained when assuming a lower than specified NA value [15,21, 22].

Table 1

Objective	Nominal aperture	Immersion	Measured aperture
UApo/340 40x	1.15	Water	1.113 ± 0.001
UPlanApo/IR 60x	1.20	Water	1.127 ± 0.003
UPlanFLN 100x&1.30	1.30	Oil	1.242 ± 0.004
PlanApo 60x	1.40	Oil	1.392 ± 0.006
PlanApo TIRFM 60x	1.45	Oil	1.439 ± 0.007

The obtained standard deviations demonstrate the high precision and repeatability of our method. The method is straightforward to implement, easy to evaluate and it should be useful for all research where precise knowledge of the NA of high-NA objectives is necessary. In theory, it could be possible to extract from images of the intensity distribution of the back focal plane also information about apodization of the objective. However, this will necessitate full knowledge of the exact orientational distribution of the molecules in the sample (which is not necessarily well-defined for spin-coated layers) and much better signal-to-noise ratio than that achieved in our measurements.

In conclusion, some limitations of the proposed method should be mentioned. Firstly, it relies on the comparison of ρ_{max} with ρ_{TIR}. Thus, if the numerical aperture of an objective is smaller than one, no total internal reflection can occur and ρ_{TIR} can not be determined. Thus, out method is limited to objectives with NA > 1. Secondly, Eq.(3) is only true as long as there is a strict linear relationship between emission angle in sample space and exit radius in the back focal plane of the objective (generalized Abbe's sine condition). If an objective shows significant aberrations, or if the used immersion medium between objective and coverslide has an incorrect refractive index, Abbe's sine condition no longer holds and Eq.(3) is no longer valid.

Acknowledgments

We are much obliged to Prof. U. Benjamin Kaupp for his generous support of our work. Conor Burke is acknowledged for helpful discussions. Luru Dai thanks the Forschungszentrum Jülich for financing his stay at this research institution. Financial support by the Deutsche Forschungsgemeinschaft and the Science Foundation of Ireland is gratefully acknowledged.